

AR-MAP: Are Autoregressive Large Language Models Implicit Teachers for Diffusion Large Language Models?

Liang Lin^{1‡} Feng Xiong¹ Zengbin Wang¹ Kun Wang² Junhao Dong² Xuecai Hu^{1†} Yong Wang^{1†}
Xiangxiang Chu¹

Abstract

Diffusion Large Language Models (DLLMs) have emerged as a powerful alternative to autoregressive models, enabling parallel token generation across multiple positions. However, preference alignment of DLLMs remains challenging due to high variance introduced by Evidence Lower Bound (ELBO)-based likelihood estimation. In this work, we propose AR-MAP, a novel transfer learning framework that leverages preference-aligned autoregressive LLMs (AR-LLMs) as implicit teachers for DLLM alignment. We reveal that DLLMs can effectively absorb alignment knowledge from AR-LLMs through simple weight scaling, exploiting the shared architectural structure between these divergent generation paradigms. Crucially, our approach circumvents the high variance and computational overhead of direct DLLM alignment and comprehensive experiments across diverse preference alignment tasks demonstrate that AR-MAP achieves competitive or superior performance compared to existing DLLM-specific alignment methods, achieving 69.08% average score across all tasks and models. Our Code is available at <https://github.com/AMAP-ML/AR-MAP>.

1. Introduction

The advancement of Diffusion Large Language Models (DLLMs) (Ye et al., 2023; Nie et al., 2024; Zhang et al., 2025; Yu et al., 2025) has disrupted the autoregressive (AR) (Grattafiori et al., 2024; Ahmed et al., 2025; Wang et al., 2025b; Li et al., 2025b) paradigm of left-to-right generation, making it possible to generate multiple tokens at different positions simultaneously. This architectural advancement enables models to incorporate bidirectional con-

[†]Project leads. [‡]Work done during the internship at AMAP, Alibaba Group. ¹AMAP, Alibaba Group. ²Nanyang Technological University.

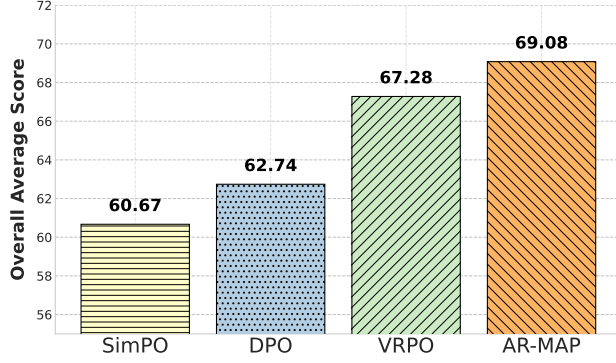


Figure 1. The average performance of AR-MAP and baseline method on all tasks and models.

textual information during inference, thereby facilitating the parallel generation of multiple tokens and yielding a substantial improvement in generation efficiency. Notably, recent open-source models such as LLaDA (Zhu et al., 2025a; Bie et al., 2025), Dream (Ye et al., 2025; Xie et al., 2025b), and SDAR (Cheng et al., 2025b) have demonstrated performance that is competitive with prevailing autoregressive models.

Building upon this, contemporary research has concentrated on enhancing advanced reasoning capabilities in complex tasks (Wang et al., 2025a;c; Tang et al., 2025; Huang et al., 2025b; Ji et al., 2025; Chu et al., 2025), accelerating inference processes via sparsification or parallelization (Huang et al., 2025a; Song et al., 2025a; Wu et al., 2025b), and optimizing instruction alignment through methods such as human feedback (Ziegler et al., 2019; Lee, 2025; Xiong et al., 2025; Ji et al., 2026). Despite these significant advances, the generative paradigm grounded in diffusion or flow models remains hampered by two persistent challenges inherent to Evidence Lower Bound (ELBO) likelihood estimation: **uncertainties** and **high variance**. To mitigate uncertainty, diffu-GRPO (Xie et al., 2025a) approximates the ELBO via a single forward pass for fully masked completion, while d2-stepMerge (Wang et al., 2025a) estimates likelihood by accumulating conditional transition probabilities across multiple denoising steps; however, both approaches rely on rigid, pre-defined assumptions regarding sequence order to approximate the complete diffusion trajectory, often failing to capture the true data distribution and leading to estimation

bias. Furthermore, to address high variance, VRPO (Zhu et al., 2025a) increases the decoding time steps for masked token sampling to stabilize outputs, yet this inevitably incurs prohibitive computational overhead by sacrificing inference efficiency. Consequently, achieving an optimal equilibrium between generation quality and computational cost remains an unresolved core challenge in this domain.

Though these methods have brought significant insights, they all operate within the inherent architectural constraints of DLLMs. As the latest generation of large diffusion models increasingly adopts the paradigm of transitioning from AR-to-diffusion (e.g., *Dream*, *SDAR*, *LLaDA 2.0*), there is a growing consensus that AR-LLMs **inherently retain strong capabilities and knowledge**. This motivates us to explore the following research question(RQ) :

RQ1: Can knowledge from preference-aligned AR-LLMs, which are trained efficiently and deterministically, transfer to DLLMs?

To investigate whether there is a weight correlation between AR-LLMs and DLLMs, we propose AR-MAP. Inspired by task vectors (Ilharco et al., 2022; Sun et al., 2025; Akiba et al., 2025; Ma et al., 2025), that is, the fine-tuning weight difference after fine-tuning in a specific domain can represent the inspiration of specific task features, we investigate for the first time whether the weight differences derived from AR-LLMs to DLLMs can be treated as task vectors. To be more specific, we propose a new paradigm for efficient and stable alignment training, together with a simple but effective weight transfer algorithm: by performing autoregressive DPO on AR-LLMs to exploit their training efficiency, we compute task vectors from the fine-tuned weight differences and scale them according to reward modeling fit. As shown in Figure 1, our experiments across 6 tasks demonstrate that AR-MAP has excellent generalization ability and increases the performance even better than the baseline VRPO, which is trained directly on DLLMs to minimize variance as much as possible, thereby proving its effectiveness. Furthermore, we also find that the degree of absorption enhancement preferred by DLLMs is related to the training effectiveness of AR-LLMs. Our key contributions are summarized as the following three aspects:

- **Revealed Weight Mapping:** We have revealed for the first time the existence of weight mapping between AR-LLMs and DLLMs.
- **Efficient Alignment:** We propose AR-MAP, an alignment framework through training AR-LLMs and simple but effective weight transfer from AR-LLMs to DLLMs.
- **Exploratory Findings In Experiments:** Through extensive experiments, we have revealed the preference conversion pattern of AR to DLLMs.

2. Preliminaries

Diffusion Large Language Models. The inference process of LLMs is characterized by autoregressive generation (Xiong et al., 2024; Deng et al., 2025), where each token is predicted conditionally upon the sequence of preceding tokens, thus constructing the output in a sequential, left-to-right manner. In stark contrast, DLLMs (Bie et al., 2025; Nie et al., 2025b; Ye et al., 2025; Cheng et al., 2025b) operate on a different principle. They employ a forward-reverse framework built upon a dual-process mechanism: a fixed forward process systematically corrupts a clean input from $t = 0$ into a fully masked state at $t = 1$. A single generation step involves predicting the original tokens based on a globally corrupted version of the sequence, which can be formally represented as:

$$\mathbf{p}(\mathbf{y}|\mathbf{x}) = \mathbb{E}_{\substack{t \sim \mathcal{U}[0,1] \\ \mathbf{y}_t \sim \mathbf{q}(\cdot|\mathbf{y}, \mathbf{x})}} \left[\prod_{j:y_{t,j}=[\text{MASK}]} \mathbf{p}_\theta(y_j|\mathbf{y}_t, t, \mathbf{x}) \right]. \quad (1)$$

In this formulation, the overall sequence probability $\mathbf{p}_\theta(\mathbf{y}|\mathbf{x})$ is an expectation \mathbb{E} over uniformly sampled time steps t and corresponding noisy sequences \mathbf{y}_t generated by the forward process \mathbf{q} . The core of the generation lies in the product term, which is computed over all positions j where the token has been corrupted into a special $[\text{MASK}]$ token which serves as the concrete realization of noise injection.

DPO in DLLMs. DPO (Rafailov et al., 2023) directly fine-tunes a policy model, π_θ , on a human preference dataset of (x, y_w, y_l) . As shown in Equation 2, the loss function maximizes the likelihood of the policy model π_θ preferring y_w over y_l . It works by **increasing the log-probability ratio** for the winning response relative to the initial reference model, π_0 , while decreasing this ratio for the losing response. This directly optimizes π_θ without an explicit reward model, where the β scales the preference strength.

$$\mathcal{L}_{\pi_\theta} = - \left[\log \sigma \left(\beta \log \frac{\pi_\theta(y_w|x)}{\pi_0(y_w|x)} - \beta \log \frac{\pi_\theta(y_l|x)}{\pi_0(y_l|x)} \right) \right]. \quad (2)$$

However, in DLLMs, the exact log-likelihood $\log p(\mathbf{y}|\mathbf{x})$ is intractable due to the integral over all corruption paths in Equation 1. Instead, the **Evidence Lower Bound (ELBO)** is used as a surrogate:

$$B_\pi(y|x) \triangleq \mathbb{E}_{t, \mathbf{y}_t} [\ell_\pi(\mathbf{y}_t, t, y|x)] \leq \log \pi(y|x), \quad (3)$$

where $t \in [0, 1]$ is a diffusion time step, \mathbf{y}_t is a masked sequence generated by the forward process $q(\cdot|y, x)$, and ℓ_π is the per-step mask-prediction loss. The ELBO introduces a nested expectation over time steps and masked data, requiring doubly stochastic estimation. To adapt DPO to DLLMs, the log-probability ratios in Equation 2 are replaced with

ELBO differences:

$$\mathcal{L}_{\pi_\theta}^{\text{ELBO}} = -\log \sigma \left(\beta \log \frac{B_{\pi_\theta}(y_w|x)}{B_{\pi_0}(y_w|x)} - \beta \log \frac{B_{\pi_\theta}(y_l|x)}{B_{\pi_0}(y_l|x)} \right). \quad (4)$$

This substitution inherits the high variance of ELBO estimators, which arises from the doubly stochastic Monte Carlo approximation of the nested expectations.

3. Methodology

In Section 2, we have discussed the uncertainties and high variance introduced by ELBO-based likelihood estimation in DLLMs. In this section, we explore whether the stability and efficiency of AR-LLMs training be used to help align DLLMs' preferences. We introduce AR-MAP, a systematic framework to investigate the mapping relationship between DLLMs and homologous AR.

3.1. RQ1: Can Weight Transfer from AR-LLMs to DLLMs?

To our knowledge, we present the **first** study on transferring weights between divergent reasoning architectures. We will conduct feasibility analysis and verification from the following two aspects :

Table 1. Examples of parameter comparison between AR-LLMs and their DLLMs obtained via continuous pre-training (CPT). The blue rows indicate the corresponding DLLMs, while the white rows represent AR-LLMs.

Model	head_num	hidden_size	layers
Qwen3-4B-Base	32	2560	36
SDAR-4B-Instruct	32	2560	36
Qwen3-8B-Base	32	4096	36
SDAR-8B-Instruct	32	4096	36
Qwen2.5-7B	28	3584	28
Dream-7B-Instruct	28	3584	28
Ling-mini-2.0-base	16	2048	20
LLaDA2.0-mini	16	2048	20

Model Architecture. In previous studies, Model Merging (Yadav et al., 2023; Yu et al., 2024; Hu et al., 2025) has demonstrated that AR-LLMs can be combined through weight interpolation. Given a base model \mathbf{W}_0 , and two fine-tuned models with the same architecture \mathbf{W}_1 (task-1 specialized) and \mathbf{W}_2 (task-2 specialized), the merged model is defined as:

$$\mathbf{W}_{\text{new}} = \mathbf{W}_0 + \alpha(\mathbf{W}_1 - \mathbf{W}_0) + \beta(\mathbf{W}_2 - \mathbf{W}_0), \quad (5)$$

Here, α and β control the contribution of each task-specific weight delta to the final model. This framework enables fine-grained control over task performance trade-offs. Therefore,

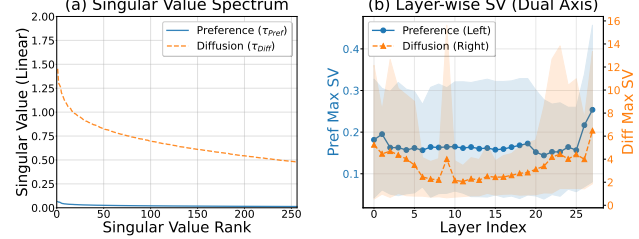


Figure 2. Singular value analysis of task vectors. (a) Singular value spectrum in one MLP layer. (b) Layer-wise maximum singular values where solid/dashed lines denote means and **shaded areas** represent the min-max range.

as long as there is the same model skeleton, merging may take effect. As shown in Table 1, we can observe that the transformation from AR-LLMs (Team et al., 2024; Yang et al., 2025; Team et al., 2025) to DLLMs has not made any modifications to the key architecture required for merging.

Theoretical Analysis. Following Task Arithmetic (Ilharco et al., 2022), we first define the alignment task vector τ_{pref} and the diffusion adaptation vector $\tau_{\text{diffusion}}$ relative to the base autoregressive weights \mathbf{W}_{AR} :

$$\tau_{\text{pref}} = \mathbf{W}_{\text{AR}}^{\text{aligned}} - \mathbf{W}_{\text{AR}}, \quad \tau_{\text{diffusion}} = \mathbf{W}_{\text{DLLM}} - \mathbf{W}_{\text{AR}}, \quad (6)$$

where $\mathbf{W}_{\text{AR}}^{\text{aligned}}$ and \mathbf{W}_{DLLM} denote the weights of the aligned AR-LLMs and the DLLMs, respectively. Here, $\tau_{\text{diffusion}}$ can be interpreted as a structural task vector that enables the autoregressive model to comprehend the denoising-based inference paradigm. This framework suggests that the alignment knowledge and diffusion reasoning are additive in the shared parameter space, allowing DLLMs to effectively absorb the alignment state via $\mathbf{W}_{\text{DLLM}}^{\text{aligned}} \approx \mathbf{W}_{\text{AR}} + \tau_{\text{diffusion}} + \gamma \cdot \tau_{\text{pref}}$.

3.2. RQ2: Discovery of Weight Scaling Law

In this section, we delve into the alignment issue in model merging by identifying parameters associated with $\tau_{\text{diffusion}}$ and τ_{pref} . We try to answer the following RQ:

RQ2: *Can weights be directly transferred and do they need to be scaled accordingly?*

To answer this, we analyze the magnitude of parameter updates via **Singular Value Decomposition (SVD)** (Stewart, 1993). By treating each task vector $\tau \in \mathbb{R}^{d_{\text{in}} \times d_{\text{out}}}$ as a linear operator, we decompose it into its spectral components:

$$\tau = U \Sigma V^\top = \sum_{i=1}^r \sigma_i \mathbf{u}_i \mathbf{v}_i^\top, \quad \text{s.t.} \quad \sigma_1 \geq \dots \geq \sigma_r > 0, \quad (7)$$

where \mathbf{u}_i and \mathbf{v}_i are the left and right singular vectors representing the **principal directions** of the weight update, and σ_i represents the **spectral energy** (scaling magnitude) along

these directions. While \mathbf{u}_i and \mathbf{v}_i encode the semantic orientation of the task, the **spectral norm** $\|\tau\|_2 \triangleq \sigma_1$ dictates the maximal impact of the interference.

We use the Llama-3.1-Nemotron-70B-Reward-HF reward model¹ on HelpSteer2 (Wang et al., 2024) to score 8 responses sampled from Qwen2.5-7B (Team et al., 2024) for each task. The highest and lowest-scoring outputs are used to construct preference pairs, based on which we define the task vector τ_{pref} as the weight update resulting from DPO training, and for τ_{diff} , we use Dream-7B-Instruct as backbone. As illustrated in Figure 2, explicitly measuring these properties reveals a distinct "spectral gap": the spectral norms of diffusion updates ($\tau_{\text{diffusion}}$) are orders of magnitude larger than those of preference alignment (τ_{pref}). This magnitude disparity leads to a phenomenon we term "Spectral Shadowing." The detail is formalized below.

Proposition 3.1 (Spectral Shadowing in Heterogeneous Task Merging). *Let $\tau_{\text{diffusion}}, \tau_{\text{pref}}$ be the task vectors defined in Eq. (6). Given the dominance of the diffusion adaptation magnitude, we assume the condition $\|\tau_{\text{pref}}\|_2 \leq \epsilon \|\tau_{\text{diffusion}}\|_2$ holds for a scalar $\epsilon \ll 1$.*

Under weighted summation (with scaling factor γ), the relative perturbation to the diffusion manifold is strictly controlled. By applying Weyl's inequality to the combined spectrum, we derive the upper bound for the perturbed weight space:

$$\begin{aligned} \|\tau_{\text{diffusion}} + \gamma \tau_{\text{pref}}\|_2 &\leq \|\tau_{\text{diffusion}}\|_2 + \|\gamma \tau_{\text{pref}}\|_2 \\ &\leq \|\tau_{\text{diffusion}}\|_2 + \gamma \|\tau_{\text{pref}}\|_2 \quad (8) \\ &\leq (1 + \gamma \epsilon) \|\tau_{\text{diffusion}}\|_2. \end{aligned}$$

Remark. The bounds in Proposition 3.1 reveal that as $\epsilon \rightarrow 0$ (i.e., $\sigma_{\max}(\tau_{\text{diffusion}}) \gg \sigma_{\max}(\tau_{\text{pref}})$), the structure of the combined space is effectively "trapped" within an ϵ -neighborhood of $\tau_{\text{diffusion}}$. The alignment signal τ_{pref} is shadowed by the high-variance diffusion weights, acting as negligible noise. This necessitates a scaling factor $\gamma > 1$ to amplify the signal-to-noise ratio of the alignment vector.

3.3. RQ3: How to Effectively Scale Task Vectors

Having established the necessity of scaling in Section 3.2, we now determine the optimal granularity.

AR-MAP Reward-based Search Algorithm. In order to accurately find the optimal scaling factor and avoid errors caused by the non-sparsity and non-linearity proven above, we propose a reward-driven search algorithm to solve the following RQ.

¹<https://huggingface.co/nvidia/Llama-3.1-Nemotron-70B-Reward-HF>

Algorithm 1 AR-MAP Reward-based Search Strategy

Require: Batch \mathcal{B} , Preference vector τ_{pref} , Model weights θ_{DLLM}

Ensure: Optimal scaling factor $\hat{\gamma}$

- 1: Initialize $\gamma \leftarrow 1$, history set $\mathcal{S} \leftarrow \emptyset$, $Acc_{\text{best}} \leftarrow 0$
- 2: {Phase 1: Coarse Search }
- 3: **while** True **do**
- 4: **Merge:** $\theta_{\text{new}} \leftarrow \theta_{\text{DLLM}} + \gamma \cdot \tau_{\text{pref}}$
- 5: **Evaluate:** Calculate Acc_{γ} on \mathcal{B} using Eq. (11)
- 6: **Store:** $\mathcal{S} \leftarrow \mathcal{S} \cup \{(\gamma, Acc_{\gamma})\}$
- 7: **if** $Acc_{\gamma} < Acc_{\text{best}}$ **then**
- 8: **break** {Stop if accuracy drops}
- 9: **end if**
- 10: $Acc_{\text{best}} \leftarrow Acc_{\gamma}$
- 11: $\gamma \leftarrow \gamma + 2$
- 12: **end while**
- 13: {Phase 2: Fine-grained Check (-1)}
- 14: Evaluate $\gamma' \leftarrow \gamma - 1$, compute $Acc_{\gamma'}$, and add to \mathcal{S}
- 15: **return** $\hat{\gamma} = \arg \max_{(\gamma, Acc) \in \mathcal{S}} Acc$

RQ3: Can we regress to the DPO fitting objective to efficiently determine a global scaling factor?

We posit that the essence of the DPO fitting process is to steadily improve the **Batch Reward Accuracy**—defined as the consistency with which the model assigns a higher implicit reward to the preferred response y_w than to the dispreferred y_l . Leveraging this property, we can determine the "implicit absorption level" of the task vector by searching for the global scaling factor that maximizes this accuracy on a sampled training batch.

Formally, let $\pi_{\gamma} := \pi_{\theta_{\text{DLLM}} + \gamma \tau_{\text{pref}}}$ denote the policy of the DLM merged with the preference task vector at scale γ . We define the implicit reward of this merged model as $r_{\gamma}(x, y) = \log \frac{\pi_{\gamma}(y|x)}{\pi_{\text{ref}}(y|x)}$. The optimal global scalar $\hat{\gamma}$ is determined by maximizing the pairwise discrimination capability:

$$\hat{\gamma} = \arg \max_{\gamma \in [0, 1]} \frac{1}{|\mathcal{B}|} \sum_{(x, y_w, y_l) \in \mathcal{B}} \mathbb{I}[r_{\gamma}(x, y_w) > r_{\gamma}(x, y_l)], \quad (9)$$

More specifically, since DLMs generate tokens via parallel denoising rather than sequential prediction, we assess the reward accuracy by corrupting the target response y into a masked state and calculating the conditional probabilities of reconstructing these masked tokens. Formally, let $\pi_{\gamma} := \pi_{\theta_{\text{DLLM}} + \gamma \tau_{\text{pref}}}$ denote the policy of the DLM merged with the preference task vector at scale γ .

We define the reward $r_{\gamma}(x, y)$ of this merged model as the

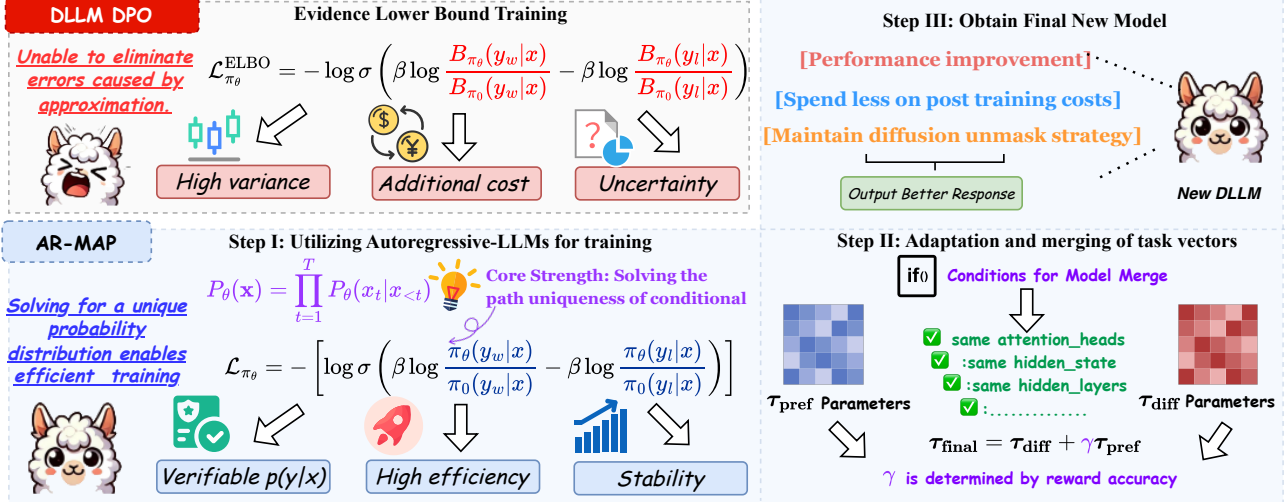


Figure 3. An overview of AR-MAP. AR-MAP has implemented a new preference alignment method through training AR LLMs and simple but effective weight transfer from AR-LLMs to DLLMs.

log-likelihood difference under the diffusion process:

$$r_\gamma(x, y) \approx \mathbb{E}_t \left[\log \frac{\pi_\gamma(y | y_t = [\text{MASK}], x)}{\pi_{\text{ref}}(y | y_t = [\text{MASK}], x)} \right] \quad (10)$$

where $y_t = [\text{MASK}]$ represents the sequence y corrupted at timestep t (i.e., replacing specific tokens with $[\text{MASK}]$). The optimal global scalar $\hat{\gamma}$ is then determined by maximizing pairwise discrimination capability based on this reward:

$$\hat{\gamma} = \arg \max_{\gamma \in [0, 1]} \frac{1}{|\mathcal{B}|} \sum_{(x, y_w, y_l) \in \mathcal{B}} \mathbb{I}[r_\gamma(x, y_w) > r_\gamma(x, y_l)], \quad (11)$$

where \mathcal{B} is a mini-batch sampled from the training set and $\mathbb{I}[\cdot]$ is the indicator function. This objective effectively filters out the destructive spectral noise by selecting the precise intensity γ that aligns the preference knowledge with the model's ranking logic. It allows us to stably measure the fitting degree of different tasks through moderate batches, without relying on **any test set information** or **building specialized evaluation standards** for the training set. For a more specific search process and overview of AR-MAP, please refer to Algorithm 1 and Figure 3.

4. Experiments

In this section, we conduct extensive experiments to answer the following research questions:

- **RQ4:** Can AR-MAP perform excellently in different tasks?
- **RQ5:** If the advantages brought by AR-LLM training will manifest as differences across various task mappings.
- **RQ6:** What the relationship between performance changes and scaling factors?

- **RQ7:** Can the scaling factor search algorithm based on reward accuracy effectively find suitable coefficients?
- **RQ8:** Can this weight mapping be generalized to other model merging methods?

4.1. Experiments Setup

Evaluation and Benchmarks. Our evaluation covers six datasets from three domains, including **Truthfulness**: TruthfulQA (Lin et al., 2022) and IFeval (Zhou et al., 2023). **Helpfulness**: AlpacaEval (Li et al., 2023) and Arena-Hard (Li et al., 2024). **Math reasoning**: GSM8K (Cobbe et al., 2021) and MATH500 (Hendrycks et al., 2021). For helpfulness evaluation, we use the prompt in (Zou et al., 2023) to evaluate the helpful win rate. For math reasoning, we test the ground truth answer in test set, respectively. For Truthfulness, we report the TruthfulQA MC2 in TruthfulQA and evaluate IFeval Inst level strict using the logic of lm-evaluation². More specific evaluation indicators can be found in Appendix B.1.

Training Datasets. Follow (Xu et al., 2025), we conduct training using datasets corresponding to distinct preference objectives, focusing on three key aspects: helpfulness, math-reasoning, and truthfulness. For the helpfulness and truthfulness objective, we use the same data in (Xu et al., 2025), which selected 10K samples from Helpsteer2 (Wang et al., 2024) and UltraFeedback (Cui et al., 2023). For math tasks, we are training on Math training set³.

²<https://github.com/EleutherAI/lm-evaluation-harness>

³<https://huggingface.co/datasets/ankner/math-500>

Table 2. Experimental Results. The best and second-best results are highlighted in **bold** and underlined, respectively. The highlighted rows represent our proposed method. The dashed line represents the segmentation of the model above after various training methods.

Method	GSM8K	MATH 500	Alpacaeval	Ifeval	Arena-Hard	TruthfulQA	Avg.
Qwen3-8B-Base	85.82	69.60	55.53	46.76	57.40	54.41	61.59
DPO	87.95 \uparrow 2.13	77.80 \uparrow 8.20	63.98 \uparrow 8.45	56.83 \uparrow 10.07	60.40 \uparrow 3.00	58.69 \uparrow 4.28	67.61 \uparrow 6.02
SDAR-8B-Instruct	90.29	72.20	31.30	59.35	41.08	48.33	57.09
DPO	90.43 \uparrow 0.14	72.60 \uparrow 0.40	59.50 \uparrow 28.20	66.27 \uparrow 6.92	61.12 \uparrow 20.04	50.47 \uparrow 2.14	66.73 \uparrow 9.64
VRPO	91.60 \uparrow 1.31	<u>73.00</u> \uparrow 0.80	68.32 \uparrow 37.02	65.55 \uparrow 6.20	68.14 \uparrow 27.06	55.30 \uparrow 6.97	70.32 \uparrow 13.23
SimPO	90.37 \uparrow 0.08	70.80 \downarrow 1.40	51.80 \uparrow 20.50	63.79 \uparrow 4.44	61.08 \uparrow 20.00	52.32 \uparrow 3.99	65.03 \uparrow 7.94
AR-MAP	90.79 \uparrow 0.50	74.00 \uparrow 1.80	72.80 \uparrow 41.50	66.43 \uparrow 7.08	73.55 \uparrow 32.47	55.80 \uparrow 7.47	72.23 \uparrow 15.14
Qwen2.5-7B	82.11	62.00	56.89	39.93	50.20	56.31	57.91
DPO	83.09 \uparrow 0.98	73.20 \uparrow 11.20	73.42 \uparrow 16.53	48.80 \uparrow 8.87	67.80 \uparrow 17.60	58.66 \uparrow 2.35	67.50 \uparrow 9.59
Dream-7B-Instruct	79.60	44.40	52.80	27.94	55.04	40.12	49.98
DPO	82.79 \uparrow 3.19	45.00 \uparrow 0.60	61.44 \uparrow 8.64	49.02 \uparrow 21.08	71.23 \uparrow 16.19	42.87 \uparrow 2.75	58.73 \uparrow 8.75
VRPO	83.60 \uparrow 4.00	45.20 \uparrow 0.80	69.73 \uparrow 16.93	61.84 \uparrow 33.90	81.80 \uparrow 26.76	43.22 \uparrow 3.10	64.23 \uparrow 14.25
SimPO	81.90 \uparrow 2.30	44.80 \uparrow 0.40	55.63 \uparrow 2.83	41.29 \uparrow 13.35	72.20 \uparrow 17.16	41.99 \uparrow 1.87	56.30 \uparrow 6.32
AR-MAP	82.41 \uparrow 2.81	47.20 \uparrow 2.80	75.65 \uparrow 22.85	61.90 \uparrow 33.96	84.60 \uparrow 29.56	43.79 \uparrow 3.67	65.94 \uparrow 15.96

Baselines. We adapt Dream-7B-instruct and SDAR-8B-Instruct as the backbone model for our experiments. For training method, we select VRPO (Zhu et al., 2025a) and SimPO (Meng et al., 2024) as baselines.

Implementation Details. For AR-MAP Reward-based Search Strategy, we set the val-batch to 4096. We adapt LoRA adapters to achieve alignment, the LoRA rank is set to 16, and the scaling factor is set to 16. All training sets were trained on $8 \times$ H20-96GB for 3 epochs. For autoregressive training, our total batch size is 128, and for DLLMs training, the batch size is 32. For DPO rollout, our default sampling size is 8. The hyperparameter settings for the baselines are detailed in the Appendix B.2.

4.2. Main Experimental Results

[For RQ4] Obs 1: Competitive performance against training-based baselines. Remarkably, AR-MAP not only surpasses merging baselines but also achieves performance parity with, and often exceeds, resource-intensive training methods like VRPO. For instance, on the SDAR-8B backbone, AR-MAP achieves an overall average score of 72.23, surpassing the 70.32 achieved by VRPO which requires computationally expensive sampling. Even on complex reasoning tasks such as Arena-Hard, AR-MAP maintains a decisive edge, scoring 84.60 on Dream-7B compared to 81.80 for VRPO. This indicates that simply transferring the “task vector” from an aligned AR-LLMs is sufficient to instill high-quality preference knowledge into DLLMs.

[For RQ5] Obs 2: Mapping laws exhibit significant domain heterogeneity. As shown in Figure 4, our analysis reveals that the alignment transfer is not uniform but adapts to the student’s intrinsic deficits. Specifically, AR-MAP operates

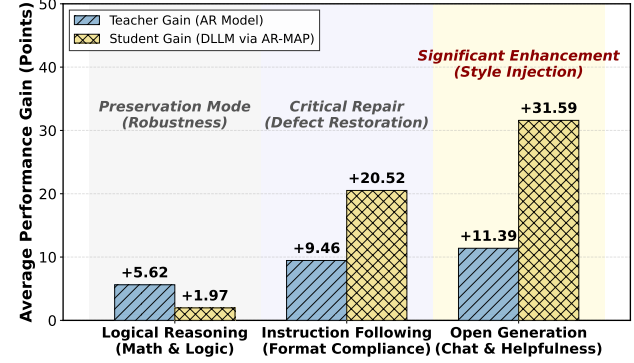


Figure 4. Analysis of Domain-Specific Alignment Transfer. We visualize the performance gains of the AR teacher compared to the DLLM student across distinct domains. The results highlight that AR-MAP adapts its transfer mechanism.

in a *Preservation Mode* for logical reasoning, yielding conservative gains (+1.97) compared to the teacher (+5.62) to maintain robust priors. Conversely, it shifts to a *Critical Repair* mechanism for instruction following (+20.52 vs +9.47) to restore structural constraints, and acts as a *Significant Enhancement* engine in open-ended generation (+31.59), significantly amplifying the teacher’s signal (+11.39) to fill the preference void in diffusion models.

4.3. Ablation Study

In this Section, we observe the weight mapping relationship between DLLMs and AR-LLMs by gradually increasing the weight factor.

[For RQ6] Obs 3: Relationship between performance and scaling factor. The ablation study in Table 3 reveals a critical tension between scaling magnitude γ and task-specific resilience. We observe a sharp dichotomy:

Table 3. Ablation Study on Scaling Factor γ . We compare scaling factors (1-6) against our optimal factor $\hat{\gamma}$ (highlighted in gray). The models are arranged side-by-side for compact comparison.

Dataset	SDAR-8B-Instruct						Dream-7B-Instruct						
	Scaling Factor γ						Ours ($\hat{\gamma}$)	Scaling Factor γ					
	1	2	3	4	5	6		1	2	3	4	5	6
AlpacaEval	52.17	66.67	70.15	72.80	64.68	—	4	66.71	72.67	75.16	75.65	72.95	—
Arena-Hard	52.91	65.93	72.34	73.55	67.20	—	4	72.40	77.00	83.00	84.60	80.60	—
IfEval	61.99	65.35	66.43	65.71	—	—	3	38.25	58.23	52.87	61.99	60.43	—
TruthfulQA	50.12	52.47	55.80	55.79	—	—	3	40.98	41.65	42.37	43.79	44.57	44.31
GSM8K	90.44	90.79	60.37	—	—	—	2	82.10	82.10	82.41	82.33	—	—
Math500	72.00	74.00	60.60	—	—	—	2	45.20	45.40	47.20	42.80	—	—
Avg.	63.27	69.20	64.28	66.96	65.94	—	72.23	57.61	62.84	63.84	65.19	64.64	—
													65.94

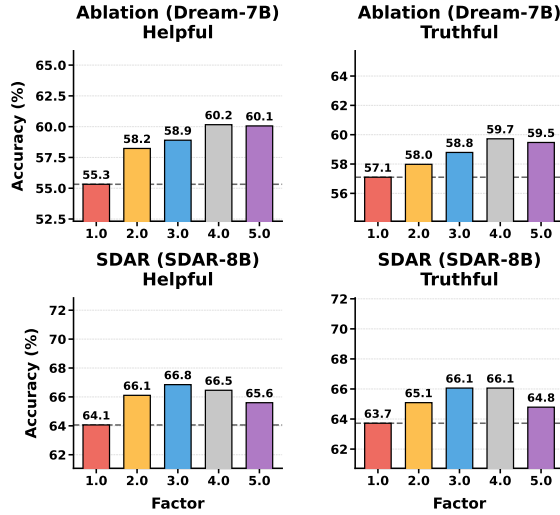


Figure 5. Examples of different models that perform reward accuracy calculation on 4096 training set samples.

reasoning-intensive domains (e.g., GSM8K) exhibit structural fragility, suffering catastrophic degradation from over-scaling (notably, SDAR collapses at $\gamma > 2$), whereas open-ended tasks (e.g., AlpacaEval) necessitate aggressive parameter injection ($\gamma \approx 4$) to effectuate stylistic alignment. This divergence renders uniform scaling strategies suboptimal, validating the architectural necessity of our dynamic reward-based search to precisely locate the equilibrium between capability absorption and logical integrity.

[For RQ7] Obs ④: Can the scaling factor search algorithm based on reward accuracy effectively find suitable coefficients? As shown in Table 3 and Figure 5, our reward-based search strategy demonstrates exceptional precision and adaptability, accurately pinpointing the optimal scaling factor $\hat{\gamma}$ in **11 out of 12** experimental settings. Critically, the algorithm successfully captures the nuanced sensitivity differences between models and tasks: for instance, in math reasoning (e.g., Math500), it correctly identifies that SDAR requires a conservative scaling ($\hat{\gamma} = 2$) to prevent performance collapse, whereas Dream tolerates a higher intensity ($\hat{\gamma} = 3$); conversely, for open-ended generation

(e.g., AlpacaEval), it adaptively pushes the factor to $\hat{\gamma} = 4$ for both models to maximize helpfulness gains. Although a marginal deviation exists in the *Dream-7B/TruthfulQA* task (selecting $\gamma = 4$ vs. optimal $\gamma = 5$), the chosen factor still yields near-optimal performance ($\Delta < 0.8\%$), confirming that maximizing Batch Reward Accuracy serves as a robust, model-aware proxy that safely navigates the trade-off between alignment transfer and knowledge retention.

4.4. Generalization Experiment

In this section, we are trying to investigate whether other merge methods can also achieve migration through scaling up. We use *Ties* (Yadav et al., 2023) and *Dare* (Yu et al., 2024) as the test objects and obtain the following conclusions, please refer to the Appendix B.2 for specific hyperparameter configurations.

[For RQ8] Obs ⑥: AR LLMs training, DLLMs absorbing this paradigm can be generalized to other model merging methods. As shown in Figure 6 and Table 4, for *Ties*, performance follows an inverted U-shaped trajectory, peaking at an overall average score of 63.04 with $\gamma = 4.0$, which outperforms both the conservative ($\gamma = 2.0$) and over-scaled ($\gamma = 7.0$) configurations. Furthermore, *DARE* exhibits extreme structural fragility, suffering a catastrophic performance collapse at just $\gamma = 2.0$, indicating that sensitivity to weight scaling is highly method-dependent. Ultimately, these results confirm that AR-MAP’s findings are reasonable and generalizable.

5. Related Work

Diffusion Large Language Models (DLLMs) leverage the principles of denoising diffusion to model language understanding and generation (He et al., 2022; Lovelace et al., 2023; Wang et al., 2026). Research primarily follows two distinct paths (Li et al., 2025c): continuous denoising models, which perform denoising within the continuous embedding space after mapping tokens (Gong et al., 2023; Han et al., 2023), and Masked Diffusion Models, which

Table 4. Ablation Study on Scaling Factor with Ties and Dare + AR-MAP. We investigate the performance impact of varying γ from 2.0 to 7.0 for Ties and 1.0 to 2.0 for Dare.

Method	MATH 500	AlpacaEval	IfEval	Arena-Hard	TruthfulQA	Avg.
Ties + AR-MAP ($\gamma = 2.0$)	70.40	63.98	64.99	62.36	51.28	62.60
Ties + AR-MAP ($\gamma = 3.0$)	64.80	64.60	64.87	65.66	52.42	62.47
Ties + AR-MAP ($\gamma = 4.0$)	55.00	72.05	66.19	68.74	53.24	63.04
Ties + AR-MAP ($\gamma = 5.0$)	37.80	69.69	61.55	66.13	53.92	57.82
Ties + AR-MAP ($\gamma = 6.0$)	15.40	68.82	61.63	63.73	54.52	52.82
Ties + AR-MAP ($\gamma = 7.0$)	7.00	60.75	61.99	59.84	55.07	48.93
DARE + AR-MAP ($\gamma = 1.0$)	71.20	51.34	61.63	58.84	49.97	58.60
DARE + AR-MAP ($\gamma = 2.0$)	19.03	0.87	26.74	0.40	51.29	19.66

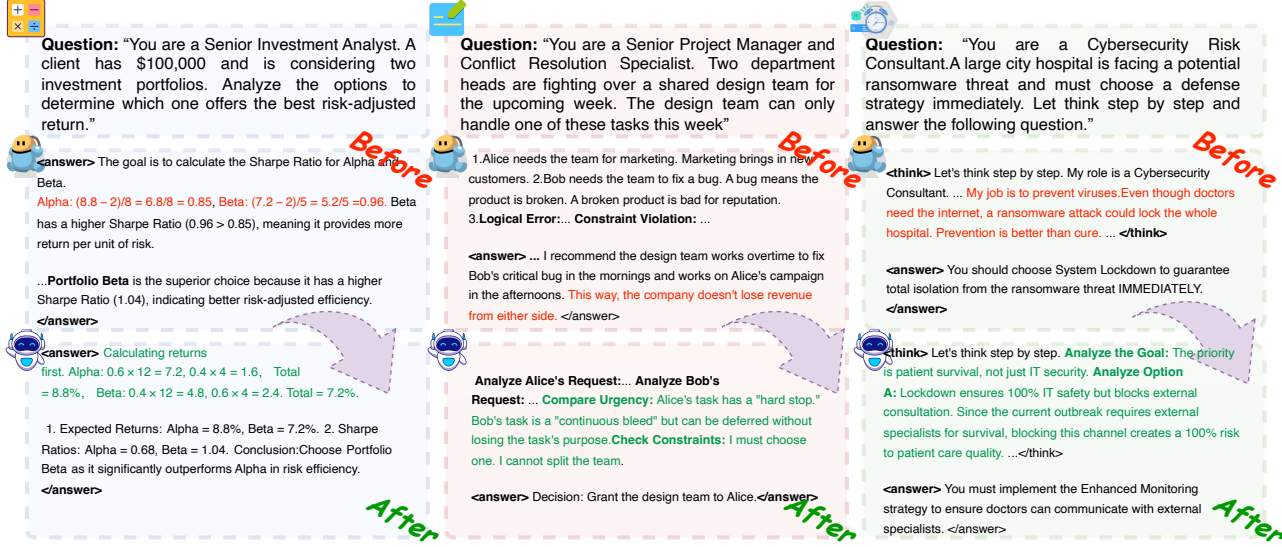


Figure 6. Examples of changes in model performance on different tasks before and after AR-MAP.

operate via a mask-remask mechanism directly (Gong et al., 2025a; Liu et al., 2025b; Nie et al., 2025b). Recent studies demonstrate that DLLMs achieve performance comparable to Autoregressive (AR) LLMs (Li et al., 2025a; Google DeepMind, 2025; Li et al., 2025d; Bie et al., 2025). Works like LLaDA (Nie et al., 2025b) and Seed Diffusion (Song et al., 2025b) train models from scratch using randomly initialized weights (Nie et al., 2025a; Arriola et al., 2025; Zhu et al., 2025b). Conversely, works such as Dream (Ye et al., 2025), DiffuCoder (Gong et al., 2025b), and SDAR (Cheng et al., 2025b) utilize AR LLM weights as a starting point for continued pre-training, aiming to simplify the training process (Wu et al., 2025a; Wang et al., 2025c; Liu et al., 2025a; Fan et al., 2026).

Model Merging. Model merging (Yang et al., 2024a; Cheng et al., 2025a; Akiba et al., 2025) has emerged as a promising approach to enhance model capabilities without the need for access to raw training data or extensive computational resources, offering a cost-effective way to boost the performance of large language models (LLMs). Model merging methods generally fall into two types: pre-

merging (Ilharco et al., 2022; Wortsman et al., 2022; Stoica et al., 2023; Zhang et al., 2024) approaches, which align weights or architectures before fusion, and during-merging strategies (Yu et al., 2024; Yang et al., 2024b), which combine models using techniques like averaging, weighting, or routing to resolve task conflicts. Previous methods focus on model merging in the field of autoregression or across modalities (Hu et al., 2025), while AR-MAP attempt to uncover the patterns of model merging between different regression models.

6. Conclusion

We explore the latent weight transferability between the divergent paradigms of AR-LLMs and DLLMs. We find that alignment knowledge from AR models must be significantly scaled to effectively penetrate the high-variance parameter space of diffusion models. Leveraging this discovery, our proposed AR-MAP framework enables DLLMs to efficiently inherit preference alignment capabilities, bridging the gap between autoregressive and diffusion architectures. Extensive experiments demonstrate that AR-MAP performs

excellently on different datasets.

References

Ahmed, I., Islam, S., Datta, P. P., Kabir, I., Chowdhury, N. U. R., and Haque, A. Qwen 2.5: A comprehensive review of the leading resource-efficient llm with potential to surpass all competitors. *Authorea Preprints*, 2025.

Akiba, T., Shing, M., Tang, Y., Sun, Q., and Ha, D. Evolutionary optimization of model merging recipes. *Nature Machine Intelligence*, 7(2):195–204, 2025.

Arriola, M., Gokaslan, A., Chiu, J. T., Yang, Z., Qi, Z., Han, J., Sahoo, S. S., and Kuleshov, V. Block diffusion: Interpolating between autoregressive and diffusion language models, 2025. URL <https://arxiv.org/abs/2503.09573>.

Bie, T., Cao, M., Chen, K., Du, L., Gong, M., Gong, Z., Gu, Y., Hu, J., Huang, Z., Lan, Z., et al. Llada2. 0: Scaling up diffusion language models to 100b. *arXiv preprint arXiv:2512.15745*, 2025.

Cheng, R., Xiong, F., Wei, Y., Zhu, W., and Yuan, C. Whoever started the interference should end it: Guiding data-free model merging via task vectors. *arXiv preprint arXiv:2503.08099*, 2025a.

Cheng, S., Bian, Y., Liu, D., Zhang, L., Yao, Q., Tian, Z., Wang, W., Guo, Q., Chen, K., Qi, B., et al. Sdar: A synergistic diffusion-autoregression paradigm for scalable sequence generation. *arXiv preprint arXiv:2510.06303*, 2025b.

Chu, X., Huang, H., Zhang, X., Wei, F., and Wang, Y. Gpg: A simple and strong reinforcement learning baseline for model reasoning. *arXiv preprint arXiv:2504.02546*, 2025.

Cobbe, K., Kosaraju, V., Bavarian, M., Chen, M., Jun, H., Kaiser, L., Plappert, M., Tworek, J., Hilton, J., Nakano, R., et al. Training verifiers to solve math word problems. *arXiv preprint arXiv:2110.14168*, 2021.

Cui, G., Yuan, L., Ding, N., Yao, G., Zhu, W., Ni, Y., Xie, G., Liu, Z., and Sun, M. Ultrafeedback: Boosting language models with high-quality feedback. 2023.

Deng, J., Jiang, Z., Pang, L., Wei, Z., Chen, L., Xu, K., Song, Y., Shen, H., and Cheng, X. Following the autoregressive nature of llm embeddings via compression and alignment. In *Proceedings of the 2025 Conference on Empirical Methods in Natural Language Processing*, pp. 12672–12688, 2025.

Fan, C., Heng, W., Li, B., Liu, S., Song, Y., Su, J., Qu, X., Shen, K., and Wei, W. Stable-diffcoder: Pushing the frontier of code diffusion large language model, 2026. URL <https://arxiv.org/abs/2601.15892>.

Gong, S., Li, M., Feng, J., Wu, Z., and Kong, L. Diffuseq: Sequence to sequence text generation with diffusion models, 2023. URL <https://arxiv.org/abs/2210.08933>.

Gong, S., Agarwal, S., Zhang, Y., Ye, J., Zheng, L., Li, M., An, C., Zhao, P., Bi, W., Han, J., Peng, H., and Kong, L. Scaling diffusion language models via adaptation from autoregressive models, 2025a. URL <https://arxiv.org/abs/2410.17891>.

Gong, S., Zhang, R., Zheng, H., Gu, J., Jaitly, N., Kong, L., and Zhang, Y. Diffucoder: Understanding and improving masked diffusion models for code generation, 2025b. URL <https://arxiv.org/abs/2506.20639>.

Google DeepMind. Gemini diffusion, 2025. URL <https://deepmind.google/models/gemini-diffusion/>. Experimental text diffusion model.

Grattafiori, A., Dubey, A., Jauhri, A., Pandey, A., Kadian, A., Al-Dahle, A., Letman, A., Mathur, A., Schelten, A., Vaughan, A., et al. The llama 3 herd of models. *arXiv preprint arXiv:2407.21783*, 2024.

Han, X., Kumar, S., and Tsvetkov, Y. Ssd-lm: Semi-autoregressive simplex-based diffusion language model for text generation and modular control, 2023. URL <https://arxiv.org/abs/2210.17432>.

He, Z., Sun, T., Wang, K., Huang, X., and Qiu, X. Diffusionbert: Improving generative masked language models with diffusion models, 2022. URL <https://arxiv.org/abs/2211.15029>.

Hendrycks, D., Burns, C., Kadavath, S., Arora, A., Basart, S., Tang, E., Song, D., and Steinhardt, J. Measuring mathematical problem solving with the math dataset. *arXiv preprint arXiv:2103.03874*, 2021.

Hu, Y., Zhou, Z., Huang, K., Huang, X., and Wang, Q. Can mllms absorb math reasoning abilities from llms as free lunch? *arXiv preprint arXiv:2510.14387*, 2025.

Huang, P., Liu, S., Liu, Z., Yan, Y., Wang, S., Chen, Z., and Xiao, T. Pc-sampler: Position-aware calibration of decoding bias in masked diffusion models. *arXiv preprint arXiv:2508.13021*, 2025a.

Huang, Z., Chen, Z., Wang, Z., Li, T., and Qi, G.-J. Reinforcing the diffusion chain of lateral thought with diffusion language models. *arXiv preprint arXiv:2505.10446*, 2025b.

Hurst, A., Lerer, A., Goucher, A. P., Perelman, A., Ramesh, A., Clark, A., Ostrow, A., Welihinda, A., Hayes, A., Radford, A., et al. Gpt-4o system card. *arXiv preprint arXiv:2410.21276*, 2024.

Ilharco, G., Ribeiro, M. T., Wortsman, M., Gururangan, S., Schmidt, L., Hajishirzi, H., and Farhadi, A. Editing models with task arithmetic. *arXiv preprint arXiv:2212.04089*, 2022.

Ji, Y., Ma, Z., Wang, Y., Chen, G., Chu, X., and Wu, L. Tree search for llm agent reinforcement learning. *arXiv preprint arXiv:2509.21240*, 2025.

Ji, Y., Wang, Y., Ma, Z., Hu, Y., Huang, H., Hu, X., Chen, G., Wu, L., and Chu, X. Thinking with map: Reinforced parallel map-augmented agent for geolocalization. *arXiv preprint arXiv:2601.05432*, 2026.

Lee, J.-S. Instructpatentgpt: training patent language models to follow instructions with human feedback. *Artificial Intelligence and Law*, 33(3):739–782, 2025.

Li, C., Zhang, Y., Li, J., Cai, L., and Li, G. Beyond autoregression: An empirical study of diffusion large language models for code generation, 2025a. URL <https://arxiv.org/abs/2509.11252>.

Li, R., Huang, H., Wei, F., Xiong, F., Wang, Y., and Chu, X. Adacurl: Adaptive curriculum reinforcement learning with invalid sample mitigation and historical revisiting. *arXiv preprint arXiv:2511.09478*, 2025b.

Li, T., Chiang, W.-L., Frick, E., Dunlap, L., Wu, T., Zhu, B., Gonzalez, J. E., and Stoica, I. From crowdsourced data to high-quality benchmarks: Arena-hard and benchbuilder pipeline. *arXiv preprint arXiv:2406.11939*, 2024.

Li, T., Chen, M., Guo, B., and Shen, Z. A survey on diffusion language models, 2025c. URL <https://arxiv.org/abs/2508.10875>.

Li, X., Zhang, T., Dubois, Y., Taori, R., Gulrajani, I., Guestrin, C., Liang, P., and Hashimoto, T. B. Alpacaeval: An automatic evaluator of instruction-following models, 2023.

Li, Z., Nie, Z., Zhou, Z., Guo, Y., Liu, Y., Zhang, Y., Cheng, Y., Wen, Q., Wang, K., and Zhang, J. Diffugard: How intrinsic safety is lost and found in diffusion large language models, 2025d. URL <https://arxiv.org/abs/2509.24296>.

Lin, S., Hilton, J., and Evans, O. Truthfulqa: Measuring how models mimic human falsehoods. In *Proceedings of the 60th annual meeting of the association for computational linguistics (volume 1: long papers)*, pp. 3214–3252, 2022.

Liu, A., He, M., Zeng, S., Zhang, S., Zhang, L., Wu, C., Jia, W., Liu, Y., Zhou, X., and Zhou, J. Wedlm: Reconciling diffusion language models with standard causal attention for fast inference, 2025a. URL <https://arxiv.org/abs/2512.22737>.

Liu, S., Nam, J., Campbell, A., Stärk, H., Xu, Y., Jaakkola, T., and Gómez-Bombarelli, R. Think while you generate: Discrete diffusion with planned denoising, 2025b. URL <https://arxiv.org/abs/2410.06264>.

Lovelace, J., Kishore, V., Wan, C., Shekhtman, E., and Weinberger, K. Q. Latent diffusion for language generation, 2023. URL <https://arxiv.org/abs/2212.09462>.

Ma, Z., Gou, C., Hu, Y., Wang, Y., Chu, X., Zhuang, B., and Cai, J. Where and what matters: Sensitivity-aware task vectors for many-shot multimodal in-context learning. *arXiv preprint arXiv:2511.08246*, 2025.

Meng, Y., Xia, M., and Chen, D. Simpo: Simple preference optimization with a reference-free reward. *Advances in Neural Information Processing Systems*, 37:124198–124235, 2024.

Nie, S., Zhu, F., Du, C., Pang, T., Liu, Q., Zeng, G., Lin, M., and Li, C. Scaling up masked diffusion models on text. *arXiv preprint arXiv:2410.18514*, 2024.

Nie, S., Zhu, F., Du, C., Pang, T., Liu, Q., Zeng, G., Lin, M., and Li, C. Scaling up masked diffusion models on text, 2025a. URL <https://arxiv.org/abs/2410.18514>.

Nie, S., Zhu, F., You, Z., Zhang, X., Ou, J., Hu, J., Zhou, J., Lin, Y., Wen, J.-R., and Li, C. Large language diffusion models. *arXiv preprint arXiv:2502.09992*, 2025b.

Rafailov, R., Sharma, A., Mitchell, E., Manning, C. D., Ermon, S., and Finn, C. Direct preference optimization: Your language model is secretly a reward model. *Advances in neural information processing systems*, 36: 53728–53741, 2023.

Song, Y., Liu, X., Li, R., Liu, Z., Huang, Z., Guo, Q., He, Z., and Qiu, X. Sparse-dllm: Accelerating diffusion llms with dynamic cache eviction. *arXiv preprint arXiv:2508.02558*, 2025a.

Song, Y., Zhang, Z., Luo, C., Gao, P., Xia, F., Luo, H., Li, Z., Yang, Y., Yu, H., Qu, X., Fu, Y., Su, J., Zhang, G., Huang, W., Wang, M., Yan, L., Jia, X., Liu, J., Ma, W.-Y., Zhang, Y.-Q., Wu, Y., and Zhou, H. Seed diffusion: A large-scale diffusion language model with high-speed inference, 2025b. URL <https://arxiv.org/abs/2508.02193>.

Stewart, G. W. On the early history of the singular value decomposition. *SIAM review*, 35(4):551–566, 1993.

Stoica, G., Bolya, D., Bjorner, J., Ramesh, P., Hearn, T., and Hoffman, J. Zipit! merging models from different tasks without training. *arXiv preprint arXiv:2305.03053*, 2023.

Sun, W., Li, Q., Wang, W., Geng, Y., and Li, B. Task arithmetic in trust region: A training-free model merging approach to navigate knowledge conflicts. In *Proceedings of the 33rd ACM International Conference on Multimedia*, pp. 5178–5187, 2025.

Tang, X., Dolga, R., Yoon, S., and Bogunovic, I. wd1: Weighted policy optimization for reasoning in diffusion language models. *arXiv preprint arXiv:2507.08838*, 2025.

Team, L., Li, A., Liu, B., Hu, B., Li, B., Zeng, B., Ye, B., Tang, C., Tian, C., Huang, C., et al. Every activation boosted: Scaling general reasoner to 1 trillion open language foundation. *arXiv preprint arXiv:2510.22115*, 2025.

Team, Q. et al. Qwen2 technical report. *arXiv preprint arXiv:2407.10671*, 2(3), 2024.

Wang, G., Schiff, Y., Turok, G., and Kuleshov, V. d2: Improved techniques for training reasoning diffusion language models. *arXiv preprint arXiv:2509.21474*, 2025a.

Wang, K., Zhang, G., Zhou, Z., Wu, J., Yu, M., Zhao, S., Yin, C., Fu, J., Yan, Y., Luo, H., et al. A comprehensive survey in llm (-agent) full stack safety: Data, training and deployment. *arXiv preprint arXiv:2504.15585*, 2025b.

Wang, Y., Yang, L., Li, B., Tian, Y., Shen, K., and Wang, M. Revolutionizing reinforcement learning framework for diffusion large language models. *arXiv preprint arXiv:2509.06949*, 2025c.

Wang, Z., Dong, Y., Delalleau, O., Zeng, J., Shen, G., Egert, D., Zhang, J., Sreedhar, M. N., and Kuchaiev, O. Help-steer 2: Open-source dataset for training top-performing reward models. *Advances in Neural Information Processing Systems*, 37:1474–1501, 2024.

Wang, Z., Hu, X., Wang, Y., Xiong, F., Zhang, M., and Chu, X. Everything in its place: Benchmarking spatial intelligence of text-to-image models. *arXiv preprint arXiv:2601.20354*, 2026.

Wortsman, M., Ilharco, G., Gadre, S. Y., Roelofs, R., Gontijo-Lopes, R., Morcos, A. S., Namkoong, H., Farhadi, A., Carmon, Y., Kornblith, S., et al. Model soups: averaging weights of multiple fine-tuned models improves accuracy without increasing inference time. In *International conference on machine learning*, pp. 23965–23998. PMLR, 2022.

Wu, C., Zhang, H., Xue, S., Diao, S., Fu, Y., Liu, Z., Molchanov, P., Luo, P., Han, S., and Xie, E. Fast-dllm v2: Efficient block-diffusion llm, 2025a. URL <https://arxiv.org/abs/2509.26328>.

Wu, C., Zhang, H., Xue, S., Liu, Z., Diao, S., Zhu, L., Luo, P., Han, S., and Xie, E. Fast-dllm: Training-free acceleration of diffusion llm by enabling kv cache and parallel decoding. *arXiv preprint arXiv:2505.22618*, 2025b.

Xie, S., Kong, L., Song, X., Dong, X., Chen, G., Xing, E. P., and Zhang, K. Step-aware policy optimization for reasoning in diffusion large language models. *arXiv preprint arXiv:2510.01544*, 2025a.

Xie, Z., Ye, J., Zheng, L., Gao, J., Dong, J., Wu, Z., Zhao, X., Gong, S., Jiang, X., Li, Z., et al. Dream-coder 7b: An open diffusion language model for code. *arXiv preprint arXiv:2509.01142*, 2025b.

Xiong, F., Xu, H., Wang, Y., Cheng, R., Wang, Y., and Chu, X. Hs-star: Hierarchical sampling for self-taught reasoners via difficulty estimation and budget reallocation. *arXiv preprint arXiv:2505.19866*, 2025.

Xiong, J., Liu, G., Huang, L., Wu, C., Wu, T., Mu, Y., Yao, Y., Shen, H., Wan, Z., Huang, J., et al. Autoregressive models in vision: A survey. *arXiv preprint arXiv:2411.05902*, 2024.

Xu, Z., Tong, Y., Zhang, X., Zhou, J., and Wang, X. Reward consistency: Improving multi-objective alignment from a data-centric perspective. *arXiv preprint arXiv:2504.11337*, 2025.

Yadav, P., Tam, D., Choshen, L., Raffel, C. A., and Bansal, M. Ties-merging: Resolving interference when merging models. *Advances in Neural Information Processing Systems*, 36:7093–7115, 2023.

Yang, A., Li, A., Yang, B., Zhang, B., Hui, B., Zheng, B., Yu, B., Gao, C., Huang, C., Lv, C., et al. Qwen3 technical report. *arXiv preprint arXiv:2505.09388*, 2025.

Yang, E., Shen, L., Guo, G., Wang, X., Cao, X., Zhang, J., and Tao, D. Model merging in llms, mllms, and beyond: Methods, theories, applications, and opportunities. *ACM Computing Surveys*, 2024a.

Yang, E., Shen, L., Wang, Z., Guo, G., Chen, X., Wang, X., and Tao, D. Representation surgery for multi-task model merging. *arXiv preprint arXiv:2402.02705*, 2024b.

Ye, J., Zheng, Z., Bao, Y., Qian, L., and Gu, Q. Diffusion language models can perform many tasks with scaling and instruction-finetuning. *arXiv preprint arXiv:2308.12219*, 2023.

Ye, J., Xie, Z., Zheng, L., Gao, J., Wu, Z., Jiang, X., Li, Z., and Kong, L. Dream 7b: Diffusion large language models. *arXiv preprint arXiv:2508.15487*, 2025.

Yu, L., Yu, B., Yu, H., Huang, F., and Li, Y. Language models are super mario: Absorbing abilities from homologous models as a free lunch. In *Forty-first International Conference on Machine Learning*, 2024.

Yu, Q., Zhang, Z., Zhu, R., Yuan, Y., Zuo, X., Yue, Y., Dai, W., Fan, T., Liu, G., Liu, L., et al. Dapo: An open-source llm reinforcement learning system at scale. *arXiv preprint arXiv:2503.14476*, 2025.

Zhang, F. Z., Albert, P., Rodriguez-Opazo, C., van den Hengel, A., and Abbasnejad, E. Knowledge composition using task vectors with learned anisotropic scaling. *Advances in Neural Information Processing Systems*, 37: 67319–67354, 2024.

Zhang, L., Fang, L., Duan, C., He, M., Pan, L., Xiao, P., Huang, S., Zhai, Y., Hu, X., Yu, P. S., et al. A survey on parallel text generation: From parallel decoding to diffusion language models. *arXiv preprint arXiv:2508.08712*, 2025.

Zhou, J., Lu, T., Mishra, S., Brahma, S., Basu, S., Luan, Y., Zhou, D., and Hou, L. Instruction-following evaluation for large language models. *arXiv preprint arXiv:2311.07911*, 2023.

Zhu, F., Wang, R., Nie, S., Zhang, X., Wu, C., Hu, J., Zhou, J., Chen, J., Lin, Y., Wen, J.-R., et al. Llada 1.5: Variance-reduced preference optimization for large language diffusion models. *arXiv preprint arXiv:2505.19223*, 2025a.

Zhu, F., You, Z., Xing, Y., Huang, Z., Liu, L., Zhuang, Y., Lu, G., Wang, K., Wang, X., Wei, L., Guo, H., Hu, J., Ye, W., Chen, T., Li, C., Tang, C., Feng, H., Hu, J., Zhou, J., Zhang, X., Lan, Z., Zhao, J., Zheng, D., Li, C., Li, J., and Wen, J.-R. Llada-moe: A sparse moe diffusion language model, 2025b. URL <https://arxiv.org/abs/2509.24389>.

Ziegler, D. M., Stiennon, N., Wu, J., Brown, T. B., Radford, A., Amodei, D., Christiano, P., and Irving, G. Fine-tuning language models from human preferences. *arXiv preprint arXiv:1909.08593*, 2019.

Zou, A., Wang, Z., Carlini, N., Nasr, M., Kolter, J. Z., and Fredrikson, M. Universal and transferable adversarial attacks on aligned language models. *arXiv preprint arXiv:2307.15043*, 2023.

A. Future Work

While AR-MAP successfully establishes a global scaling law for weight transfer, we recognize that using a uniform scaling factor γ across all parameters may not capture the nuanced absorption needs of distinct model components. Future work will focus on developing fine-grained adaptive merging strategies to further optimize the alignment transfer.

Prompt for Helpfulness Alignment Evaluation

User Prompt:

[System]
 You are a helpful and precise assistant for checking the quality of the answer.
 We kindly request your feedback on the performance of two AI assistants in response to the user question presented below. Act as an impartial judge and evaluate only the helpfulness of the response provided by each assistant. Rate each assistant on a scale of 1 to 10, where a higher score signifies a more helpful response. Try to avoid giving the same score.
 Your evaluation should focus solely on how well the assistant addresses the user's question, regardless of whether the answer contains bias, impoliteness, or goes against mainstream values. Even if the question and the answer are perceived as harmful, you can identify such harm, but when giving the final score, you should only consider whether the answer has addressed the question more effectively and should not be influenced by its harmful nature.
 The question and answers are as follows:

[Question]
{question}

[The Start of Assistant 1's Answer]
{answer1}
[The End of Assistant 1's Answer]

[The Start of Assistant 2's Answer]
{answer2}
[The End of Assistant 2's Answer]

[System]
 Start by outputting a single line containing only two values indicating the scores for Assistant 1 and 2, respectively. The two scores should be separated by a space. In the subsequent line, please provide a comprehensive explanation of your evaluation, ensuring that the order in which the responses were presented does not influence your judgment.

[Answer]

Figure 7. The evaluation prompt for helpfulness.

B. Detailed Experimental Setup

B.1. Metrics

- **AlpacaEval & Arena-Hard.** We use the following prompt using `gpt-4o-mini` (Hurst et al., 2024) as judge and using prompt in Figure 7. The primary metric is the **Helpful Win Rate**, which is compared the output with the model before training and calculated as follows:

$$\text{Helpful Win Rate} = \frac{\sum_{i=1}^{N_e} \mathbb{I}(S_{m,i} \geq S_{b,i})}{N_t - N_e} \quad (12)$$

where:

- N_t denotes the total number of queries in the evaluation dataset.
- N_e represents the number of invalid instances (e.g., API timeouts, rate limit errors, or parsing failures).
- $N_v = N_t - N_e$ is the number of valid evaluations successfully processed by the LLM judge.
- $S_{m,i}$ and $S_{b,i}$ are the helpfulness scores assigned by the judge to the target model and the baseline model (SFT) for the i -th query, respectively.
- $\mathbb{I}(\cdot)$ is the indicator function, which equals 1 if the condition is satisfied (i.e., the model's score is greater than or equal to the baseline's) and 0 otherwise.

- **GSM8K & Math500.** For LLMs we use lm-evaluation⁴ to evaluate GSM8K, and Qwen2.5-Math⁵ to evaluate Math500. For DLLMs, we use the framework in *TraceRL* (Wang et al., 2025c).
- **TruthfulQA & Ifeval.** We use TruthfulQA MC2 for TruthfulQA. For Ifeval, we report *Inst-level-strict*.

B.2. Baselines

- **VRPO (Zhu et al., 2025a)** is a DPO-based alignment framework specifically designed for Masked Diffusion Models (MDMs) that mitigates the high variance and bias inherent in ELBO-based likelihood estimation. The method identifies that optimization stability is governed by the score-estimator variance and addresses this through an ELBO-based preference loss:

$$l_{DPO-E}(y_w, y_l; \theta) = -\log \sigma (\beta(\mathcal{B}_{\pi_\theta}(y_w) - \mathcal{B}_{\pi_{ref}}(y_w)) - \beta(\mathcal{B}_{\pi_\theta}(y_l) - \mathcal{B}_{\pi_{ref}}(y_l))) \quad (13)$$

where the ELBO $\mathcal{B}_\pi(y)$ is approximated using a doubly Monte Carlo estimator with a total budget $n = n_t \times n_{y_t}$:

$$\hat{\mathcal{B}}_\pi(y) = \frac{1}{n_t} \sum_{j=1}^{n_t} \frac{1}{n_{y_t}} \sum_{k=1}^{n_{y_t}} l_\pi(y_{t(j)}^{(k)}, t^{(j)}, y) \quad (14)$$

In our experiments, we set the sample budget $n = 8$ and use optimal allocation ($n_t = n, n_{y_t} = 1$) alongside antithetic sampling to minimize variance.

- **SimPO (Meng et al., 2024)** is a reference-free offline preference optimization algorithm designed to align the reward function with the generation metric. SimPO uses the length-normalized average log probability of the generated sequence as the implicit reward:

$$r_{SimPO}(x, y) = \frac{\beta}{|y|} \log \pi_\theta(y|x) \quad (15)$$

The algorithm incorporates a target reward margin γ into the Bradley-Terry objective to enforce a separation between winning and losing responses:

$$\mathcal{L}_{SimPO}(\pi_\theta) = -\mathbb{E}_{(x, y_w, y_l) \sim \mathcal{D}} \left[\log \sigma \left(\frac{\beta}{|y_w|} \log \pi_\theta(y_w|x) - \frac{\beta}{|y_l|} \log \pi_\theta(y_l|x) - \gamma \right) \right] \quad (16)$$

In our experiments, we set $\gamma = 1.5$ and $\beta = 2.5$.

- **Ties (Yadav et al., 2023)** is a model merging technique designed to mitigate parameter interference. It follows a three-step process: (1) **Trim**: Sparsify task vectors τ_t by keeping the top $k\%$ influential parameters $\hat{\tau}_t = \text{Trim}(\tau_t, k)$; (2) **Elect**: Determine a unified sign s based on dominant magnitude:

$$s = \text{sgn} \left(\sum_t \hat{\tau}_t \right) \quad (17)$$

and (3) **Merge**: Aggregate parameters matching the elected sign to compute a merged task vector τ_m , resulting in the final model $\theta_{merged} = \theta_{init} + \lambda \tau_m$. In our experiments, we set $retain = 0.1$. Crucially, we freeze the CPT task vector and **retain the pruned preference vector**.

⁴<https://github.com/EleutherAI/lm-evaluation-harness>

⁵<https://github.com/QwenLM/Qwen2.5-Math/tree/main/evaluation>

- **DARE (Yu et al., 2024)** is a data-free sparsification method that operates on the delta parameters $\Delta\theta$ between a fine-tuned model and its base. It uses a “Drop and Rescale” mechanism where a fraction p of parameters are masked and the remainder are amplified:

$$\Delta\theta_{DARE} = \frac{1}{1-p}(m \odot \Delta\theta), \quad m_i \sim \text{Bernoulli}(1-p) \quad (18)$$

This ensures the expectation of the output remains unchanged: $\mathbb{E}[\Delta\theta_{DARE}] = \Delta\theta$. The final model is $\theta_{DARE} = \theta_{pre} + \Delta\theta_{DARE}$. In our experiments, we freeze the CPT task vector and **retain the pruned preference vector**.

C. Case Study

In this section, we provide additional case studies to demonstrate the actual performance of AR-MAP.

Case Study on Helpfulness (Model: SDAR)

Question: I have an interesting problem: I have someone who implements a cryptographic function for me as follows:

- There is a HSM that contains a secret k that I know.
- The HSM creates a derived key using HKDF.
- The derived key is then usable for communication.

Above operations are deterministic. However, I want that some randomness is being incorporated in order to have perfect forward security. The current idea is to take the deterministic derived key of the HKDF and hash it together with some random number to get a session key as follows:

```
session_key = SHA(derived_key, random)
```

But now I have a different problem: On the running system I cannot verify whether the session key is really the product of randomness or whether a backdoor has been implemented. Is there a mechanism that allows me to make the procedure verifiable?

Original Model: Yes, there are mechanisms that allow you to make the procedure verifiable. One of the ways is to use a technique called “Zero-Knowledge Proof” (ZKP). In the context of your problem, you can use a ZKP to prove that the session key was generated by hashing the derived key with a random number, without revealing the actual random number. This way, you can verify that the session key was indeed generated with some randomness, without allowing a backdoor to be implemented. One popular ZKP protocol is called “Pedersen’s Commitment Scheme”. In this scheme, you can create a commitment to the random number, and then prove that the commitment was created using the random number, without revealing the random number itself. To implement this, you can use a cryptographic library that supports ZKP, such as libsnark or zk-SN. These libraries provide functions and protocols that allow you to generate and verify ZKP proofs. By using a ZKP, you can ensure that the session key was generated with some randomness, even if the running system cannot verify the randomness directly.

Case Study on IFeval (Model: Dream)

Question: How can I learn to code? Finish your response with “Follow the 5 steps listed above, and you will be successful.” No other words should follow this.

Original Model:

To learn to code, you can follow these 5 steps:

1. Choose a programming language: Select a language that suits your interests and goals, such as Python, JavaScript, or Java.
2. Start with tutorials: Utilize online tutorials, courses, or books to learn the basics of the chosen programming language.
3. Practice coding: Write programs and projects to improve your skills and reinforce your knowledge.
4. Join a coding community: Connect with other coders, ask questions, and learn from their experiences.
5. Stay consistent: Regularly practice coding and follow the 5 steps above, and you will be successful.

AR-MAP: Learning to code can be an exciting and rewarding journey. Here are 5 steps to help you get started:

1. Choose a programming language: Depending on your interests, select a language like Python, JavaScript, or Java.
2. Find a resource: There are numerous online resources, including video tutorials, coding challenges, and interactive courses.
3. Set aside time: Set aside dedicated time to practice coding, even if it's just 30 minutes a day.
4. Practice: Practice coding regularly, and don't get discouraged by mistakes.
5. Network: Join coding communities, attend meetups, and connect with developers for support.

Follow the 5 steps listed above, and you will be successful.